Performance Analysis of LTE-Advanced Networks in Different Spectrum Bands

Fourat Haider, Erol Hepsaydir, Nicola Binucci

Hutchison 3G UK
20 Grenfell Rd, Maidenhead
SL6 1EH UK
first-name.second-name@three.co.uk

***Abstract*—Hutchison 3G under the brand name of Three launched 3rd Generation Partnership Project, 3GPP Rel 5 High Speed Downlink Packet Access (HSDPA) networks, worldwide. The HSDPA network is capable of delivering data rates up to 21 Mbps today. In Rel 7, 3GPP standardised HSPA Evolution (HSPA+) which was specified to deliver maximum user data rates up to 42 Mbps by using dual Carrier Aggregation and 64 QAM in the Downlink. Since the launch of HSDPA network in the UK, Hutchison 3G observed significant increase in the data traffic. In order to deliver Mobile BroadBand (MBB) services to its customers more efficiently, Three UK has started to focus on new technologies which have been standardised by 3GPP in Rel 8/9/10. Although Long Term Evolution (LTE) network performance was studied by other researchers, the aim of this paper is to analyse the performance of LTE Carrier Aggregation (CA) in different spectrum bands to meet the International Mobile Telecommunications Advanced (IMT-Advanced) requirements.**

I. Introduction

Convergence of mobile and internet puts pressure on mobile service providers to offer faster and more efficient mobile internet access. Today, High Speed Packet Access (HSPA) networks are delivering high volumes of data transactions. However, the growth in video downloads and the increase in data usage due to smart phones will require larger air interface bandwidths. Long Term Evolution or LTE, on the other hand, is the evolution of HSPA, which was first standardized in 3GPP Release 8 to support larger bandwidths [1]. One of the requirements of LTE was to provide higher averaged user throughput. It was specified to deliver services with high efficiency based on Internet Protocol (IP). Unlike HSPA, LTE adopts Orthogonal Frequency Division Multiple Access (OFDMA) in the downlink and Single Carrier Frequency Division Multiple Access (SC-FDMA) in the uplink direction for resource sharing among multiple users. These multiple accesses increase network capacity and user throughput because of multi-user diversity gain. One of LTE features is that the operators can select various spectrum bandwidths, e.g., 1.4, 3, 5 10, 15, and 20 MHz depending on availability. 3GPP has further extended the original proposal of LTE, which is known as LTE-Advanced [2]. LTE-Advanced can be considered as one of the prominent 4G proposals that has been specified by 3GPP in Release 10. LTE-Advanced should, however, provide a backward compatibility in terms of spectrum coexistence with Release 8 based LTE. This means that it should be possible to implement LTE-Advanced in a spectrum which is already occupied by LTE devices. Furthermore, LTE-Advanced will also use the same radio interface technology as LTE.

ITU has specified IMT-Advanced data rate requirements of up to 1 Gbps and 500 Mbps in downlink and uplink directions, respectively, using Orthogonal Frequency-Division Multiplexing (OFDM) [3]. This could be achieved in 100 MHz band spectrum. However, one of the challenges that cellular operators are facing today, especially in the UK, is to find a contiguous 100 MHz in a spectrum band which is suitable for cellular based mobile communication use, i.e., below 3 GHz. Therefore, 3GPP developed Carrier Aggregation (CA) technology in Release 10 as a potential solution for increasing the LTE bandwidth to support higher data rates as required by IMT-Advanced [4]. With LTE CA, the operators can scale the spectrum bandwidth and aggregate more than two spectrum bands. The concept of CA has already been deployed in HSPA based cellular systems, under the name Dual Carrier HSPA (DC-HSPA), to aggregate two carriers in the downlink and two in the uplink [5]. However, both carriers must be contiguous in the same spectrum band. Unlike DC-HSPA, LTE CA can aggregate non-contiguous spectrums with different bandwidths. In this paper, we will first analyse the performance of single carrier LTE with different spectrum bandwidths in various carrier frequencies. Thereafter, we will study the LTE-Advanced CA feature performance and compare it with Release 8 LTE performance in different spectrum bands.

This paper is structured as follows: Section II gives an overview about carrier aggregation. Section III highlights the network assumption that is adopted in this work and Section IV presents results of our performance analysis. Finally, section V provides the summary and the concluding remarks.

II. Carrier Aggregation

Carrier Aggregation or CA is one of the most important LTE-Advanced features that have been recently standardised by 3GPP as part of LTE Release 10 in order to satisfy the IMT-Advanced requirements. The CA feature allows the eNodeB to aggregate more than one spectrum bands in order to support high data rates in the downlink as well as uplink transmission. Each carrier component should handle independent traffics that are segmented at higher layers and then transmitted using the physical layer resources of each carrier. This will require separate link level mechanisms (e.g., Hybrid automatic repeat request HARQ) and control signaling for each carrier component.

One of the main LTE-Advanced requirements is the backward compatibility with the earlier LTE Releases, i.e., Release 8 and 9. LTE devices which do not support LTE-Advanced feature can use one of the aggregated bands. The handsets supporting the CA feature, i.e., Release 10 users, are able to use multiple spectrum bands simultaneously to send and receive data. Once a user is allocated multiple carriers i.e. 10 MHz at 800 MHz and 20 MHz at 2.6 GHz bands, the eNodeB allocates the Physical Resource Blocks (PRBs) in each carrier among the users by using opportunistic scheduling. Two types of scheduling method can be used: separated or joint scheduling method [6]. In the separated mode, the scheduling algorithm is used independently on each carrier to allocate the PRBs among the users. Whereas in joint scheme, the scheduling algorithm will be performed jointly across all carrier components.

There are two different CA configurations that can be used in LTE-Advanced based cellular system [7]. Those are:

- Continuous CA

In this mode, the available multiple spectrum bands each having 20 MHz are supposed to be adjacent to each other. For example, two 20 MHz bands are aggregated to form 40 MHz band as a single spectrum. LTE networks adopt SC-OFDMA in the uplink direction. Therefore, this mode will also be used in the LTE-Advanced uplink to preserve the single carrier property.

- Non-continuous CA

Herein, the aggregated carriers can either be non-contiguous in the same frequency band, e.g., 800MHz, (intra-band aggregation) or located in different frequency bands, e.g., 800 MHz and 2.6 GHz, (inter-band aggregation) [8]. The radio channel characteristics such as path loss, building penetration loss and Doppler shift will vary significantly at different frequency bands which cause large differences on the received power. The impact of these variations could be minimized in the scheduler through Radio Resource Management (RRM).

III. Network Assumption

In this paper, a multi-cell system that has a layout of hexagonal grid consisting of 19 sites with 3 sectors is considered. An eNodeB is located at each site location to enable the communications between the User Equipment (UE) and the network. Users are assumed to be indoor and distributed uniformly within the coverage of each cell, as shown in Fig. 1. The minimum distance between the eNodeB and the mobile user is assumed to be 50 m. Symmetric (i.e., aggregating similar bandwidth) and non-contiguous LTE CA is considered in this work. For convenience, the eNodeBs and end users are indexed by the following sets that is, $m \in \mathcal{M}$ $=\{1,...,M\}$ and $n \in \mathcal{N}$ = $\{1,...,N\}$, respectively. To support the opportunistic scheduling, the eNodeB gathers the Channel Quality Information (CQI) from all users. LTE frame structure is considered, which consists of K physical Resource Blocks (PRBs), indexed by k=1,...,K. Each PRB is regarded as twelve contiguous sub-carriers in frequency domain and seven OFDM symbol in the time domain.

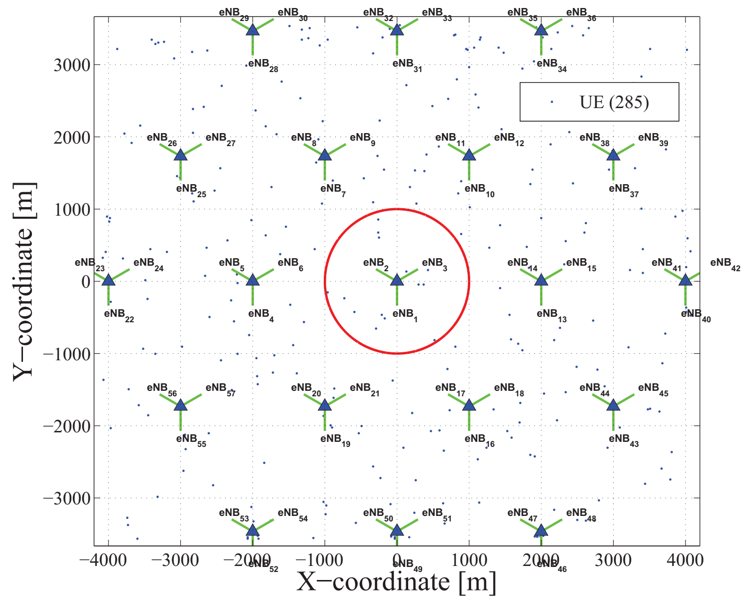

Fig. 1. A snapshot of the simulated scenario.

A. Channel Model

The path loss model is based on a generic format that is relevant to the practical scenario in urban areas. We assume that the buildings are of nearly uniform height. Hence, the path loss is calculated using

$$L(c) = L_{\mathrm{d}}(c) + L_{\mathrm{sh}} + L_{\mathrm{p}}(c) \quad [\mathrm{dB}] \qquad (1)$$

where c=1,.....,C is the carrier index. L_{d}, L_{sh}, and L_{p} are the distance dependent path losses, the shadowing losses and the frequency-dependent penetration losses. The L_{d} is assumed to be based on Okumura Hata model [9]. The shadowing loss is assumed to be log-normal distribution with zero mean and standard deviation of 8 dB.

A rayleigh channel model is used to generate a discrete time-correlated fast fading channel [10]. Thus, number of complex-valued random Gaussian variables, which is equal to the number of taps in the channel delay profile, with zero mean and unit variance are generated. These complex Gaussian values are filtered by Doppler filter, that has a frequency response of $S(f)$. The filter's output will be interpolated using a combination of a linear and polyphase algorithms. Each time delay in channel profile is then divided by the sampling time (Ts) of the system, rounded it to the nearest integer number to form a discrete-time approximation channel model. A Discrete Fourier Transform (DFT) is finally performed to get the response of the channel in the frequency domain.

B. Signal-to-Interference-plus-Noise-Ratio Analysis

The received SINR for the channel eNodeB-UE link on carrier component c in the PRB k at sub-frame t is given by

$$\text{SINR}_n^m(t,k,c) = \frac{Pl_n^m(c)|h_n^m(t,k,c)|^2}{I_{\text{oth}}(t,k,c)+N_o} \tag{2}$$

where P is the transmitted power from the serving eNodeB. $l_n^m(c)$ is the linear-valued of the $L(c)$ and $h_n^m(t,k,c)$ are the complex channel gains, and N_o is the noise power. $I_{oth}(t,k,c)$ is the received power from the interfering cells which can be calculated using the following

$$I_{\text{oth}}(t,k,c) = \sum_{q=1,q\neq m}^{M} Pl_n^q|h_n^q(k,t,c)|^2. \tag{3}$$

Now, if we assume that the channels of different cells to one particular user are changing independently, then the envelope of the combined interference variation, according to central limit theorem [11], will follow Gaussian distribution with zero mean and variance of σ^2, $N(0,\sigma^2)$. Hereby, the interference can be seen as additive white Gaussian noise, and it should be scaled appropriately. The variance of the interference σ^2 can be expressed as

$$\begin{aligned}\sigma^2 &= E[\sqrt{I_{\text{oth}}(t,k,c)}F] \\ &= \sqrt{\sum_{q=1,q\neq m}^{M} Pl(c)_n^q F^q}\end{aligned} \tag{4}$$

where F is the load factor $(0 \leq F \leq 1)$ that associated with each eNodeB [12] and $E[.]$ is the expectation operation.

C. Link level performance

Discrete adaptive modulation schemes, i.e., quaternary phase-shift keying (QPSK), 16 quadratic-amplitude modulation (QAM), and 64- QAM), are supported in this work. Coupling link and system level simulation to predict the BLER is very complex and time consuming. In this work, we use the decoupled link and system simulation approach and use preset values of link level simulation in the form of the SINR as function of Block Error Rate (BLER) for different modulation schemes to predict user throughput. The link-to-system mapping table assumed here is based on Exponential Effective SINR Mapping (EESM) [13]. The motivation behind EESM is to map the instantaneous channel quality (i.e. SINR) to a set of effective SINR_{eff}. Those SINR_{eff} are used to estimate the BLERs from a basic AWGN link level performance. The maximum effective SINR that is mapped to the target BLER is selected. Subsequently, the Modulation and Coding Scheme (MCS) is selected [13]. Hence,

$$\text{SNR}_{\text{eff}} = -\beta \log \left\{ \frac{1}{\bar{K}} \sum_{k=1}^{\bar{K}} \exp\left[\frac{-\text{SINR}_k}{\beta}\right] \right\} \tag{5}$$

where β is the calibrated factor for a given MCS, $\bar{K}$ is the number of allocated resource blocks for a particular user. Values for the parameter β for each MCS scheme, which have been derived from OFDM-based link-level simulations [14], are used in this work.

D. Spectral Efficiency Analysis

Multiuser scheduling is performed to allocated K PRBs in each carrier c to multiple users. the well-known Proportional Fair (PF) scheduling policy is considered in this work [15]. With PF, the scheduler allocates the RB k of a carrier c at time t to user $n \in \mathcal{N}$ according to the following criterion:

$$\bar{n}_k^m(t,c) = \text{arg max}_{n\in\mathcal{N}} \frac{R_n^m(k,t,c)}{\bar{R}_n^m}, \quad k = 1,...,K \tag{6}$$

$\bar{R}_n^m$ is the average delivered rate in the past, measured over a fixed window of observation. It can be calculated using an exponential average filtering. As mentioned earlier, there are two different ways to calculate the average throughput [6], either by separated scheduler or by joint scheduler. In the former method, the eNodeB will account $\bar{R}_n^m$ for each carrier, i.e.,

$$\begin{aligned}\bar{R}_n^m &= \bar{R}_n^m(t,c) \\ &= (1-\frac{1}{T})\bar{R}_n^m(t-1,c) + \frac{1}{T}\sum_{k=1}^{K} R_n^m(k,t,c)\ d_n^m(k,t,c)\end{aligned} \tag{7}$$

where T is the time window constant, $d_n(k,t,c)$ is a binary indicator that is set to 1 if the user n is scheduled on resource block k of carrier c at time t and to 0 otherwise. Whereas in the latter method, the eNodeB will calculate the average throughput over all aggregated spectrum. In other word,

$$\begin{aligned}\bar{R}_n^m &= \sum_{c=1}^{C} \bar{R}_n^m(t,c) \\ &= (1-\frac{1}{T})\bar{R}_n^m(t-1) + \frac{1}{T}\sum_{c=1}^{C}\sum_{k=1}^{K} R_n^m(k,t,c)\ d_n^m(k,t,c).\end{aligned} \tag{8}$$

As a result of that, the total cell capacity (in bps/Hz/cell) after allocating all RBs of all carriers to the selected users, can be expressed as

$$C_m(t) = \frac{1}{B}\sum_{c=1}^{C}\sum_{n=1}^{N}\sum_{k=1}^{K} R_n^m(k,t,c)\ d_n^m(k,t,c) \tag{9}$$

where B is the system bandwidth.

IV. Simulation Results and Discussion

The performance of LTE-Advanced networks in different spectrum bands is evaluated using a dynamic system level simulator which is fully compliant with 3GPP LTE specifications [1]. Monte-Carlo based simulation is performed with several iterations each having 5000 sub-frames. In each iteration mobile users are distributed independently and uniformly. The carrier bandwidths used in the simulations are 10 MHz and 20 MHz. The site-to-site distance is 3000 m (Macro 3). Statistics are gathered only in the center of the eNodeB coverage area

TABLE I
SIMULATION PARAMETERS

Parameter	Value
Transmitted power	46 dBm
Shadowing	Log-normal with 8 standard deviation
Channel model	PedB (with 6 taps)
Antenna height	25 m
Antenna gain	18 dBi
CQI delay	2 ms
TTI	1 ms
Traffic type	full buffer
Load factor (F)	1

in order to have a fair influence of interference. Other relevant simulation parameters are summarised in Table 1.

A. Single Carrier Performance Analysis

Fig. 2 compares the cell throughput of 20 MHz at 2.6 GHz with 10 MHz at 800 MHz in different load conditions. The graphs show that although the bandwidth doubles at 2.6 GHz, the cell throughput only increases 50%. This is mainly due to the higher path loss at 2.6 GHz which requires higher resources from the eNodeB.

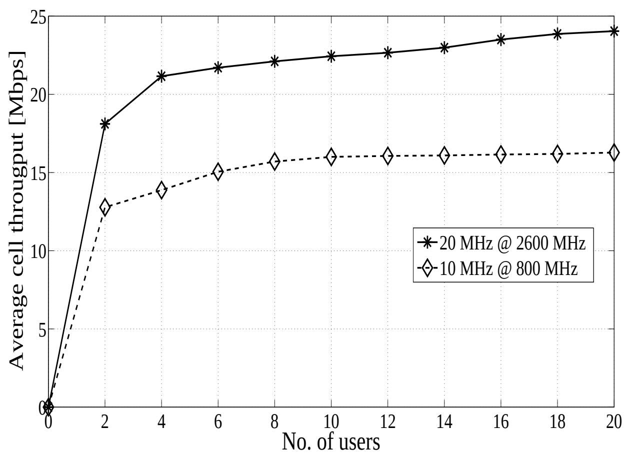

Fig. 2. Cell throughput comparison of 20 MHz and 10 MHz.

Fig. 3 compares the average spectral efficiencies of the network in both spectrum bands. As it is clearly shown, the spectral efficiency of 10 MHz at 800 MHz outperforms the 20 MHz at 2.6 GHz although it is half the bandwidth. The simulation results in individual bands show clearly that the performance of the network at the lower frequency i.e. below 1 GHz is higher than the corresponding high frequency operations i.e. 2.6 GHz. Carrier Aggregation will take advantage of both spectrum bands to improve the performance of the network i.e. higher spectral efficiency below 1 GHz and larger available bandwidths at 2.6 GHz.

B. Carrier Aggregation Performance Analysis

In this analysis we compared a single carrier of 20 MHz at 2.6 GHz LTE network based on 3GPP Rel 8 standards with

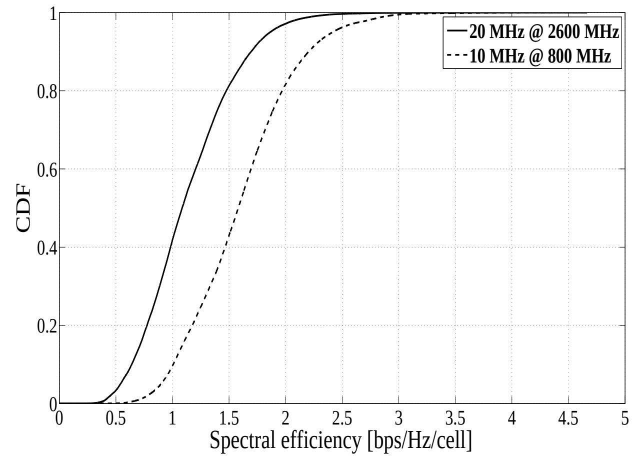

Fig. 3. CDF of spectral efficiency.

Carrier aggregation of 10 MHz at 800 MHz and 10 MHz at 2.6 GHz based on Rel 10. In this simulation, each cell was loaded with 10 users. All users are assumed to be supporting Release 10 CA feature and they can be served by both carriers. Fig. 4 shows that the cell throughput with aggregation of 10 MHz at 800 MHz and 10 MHz at 2.6 GHz is 50% higher compared to single 20 MHz carrier at 2.6 GHz due to frequency diversity.

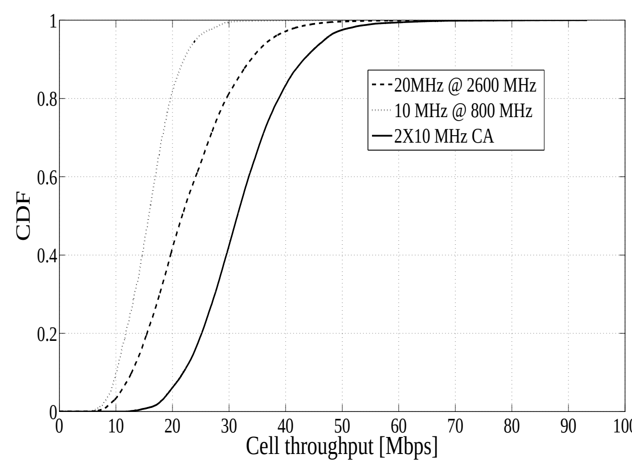

Fig. 4. CDF of cell throughput.

The user average throughput CDFs are presented in Fig 5. It can be observed that the percentage of cell edge user throughput for single carrier component of 10 MHz bandwidth at 800MHz is higher compared with 20 MHz at 2.6 GHz case. This is due to high path loss at 2.6 GHz and high building penetration loss. On the other hand, the users located near the eNodeB have higher throughput at 2.6 GHz compared with 800 MHz since they can access to larger bandwidth at good signal levels. The averaged user throughput in the coverage area was also analysed when the CA was applied, In this analysis, joint PF scheduling algorithm was used to aggregate

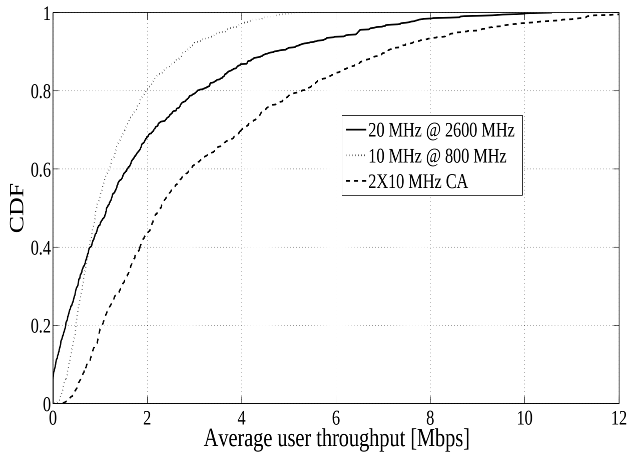

Fig. 5. CDF of user throughput.

10 MHz at 800 MHz band and 10 MHz at 2.6 GHz. As shown in Fig. 5 the user throughput CDF with CA in the coverage area is superior compared to single band operation using the same total bandwidths due to multi-diversity gain.

The average user throughput CDFs of separated and joint scheduling schemes are compared in Fig. 6 for Release 8 with 10 user. In each cell, we assume that there are 15 active users with 40% Release 10 users. Release 8 users are assigned equally in each carrier. As it is shown in Fig. 6, the Release 8 users have higher user throughput gain when joint scheduling is employed. However, Release 10 user throughput will be worse with joint scheduling algorithm. The reason is that when Release 10 users are scheduled using joint scheduling scheme, the eNodeB scheduler calculates the average throughput in past using Eq. (8) for both carriers. As a result, the fairness between Release 8 and Release 10 will increase. In case of separated scheduling, the scheduler uses an independent PF metric to allocate best PRBs in each spectrum band to all user types.

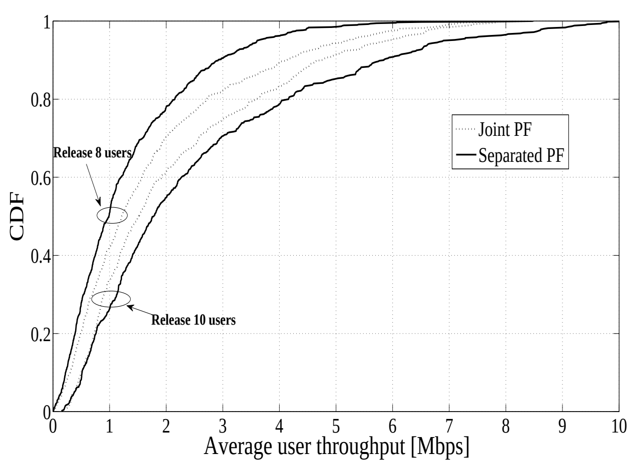

Fig. 6. CDF of user throughput.

V. Conclusions

The aim of this study was to investigate the performance of an LTE-Advanced based cellular network in different spectrum bands. We first analysed the performance of a single carrier in different bandwidths in two different spectrum bands, 800 MHz and 2.6 GHz. The simulations showed that an increased system bandwidth might not necessarily result in a higher system throughput. Hence, the simulation results demonstrated that in some cases, low frequency, i.e. 800 MHz, system was superior to a high frequency deployment i.e. 2.6 GHz although the operating bandwidth at 800 MHz was half of 2.6 GHz band. However, the deployment of CA-based system would increase the cell and user throughput significantly by extending the operating bandwidth in the network. Therefore, LTE-Advance is a strong candidate to deliver IMT-Advanced requirements. However, the increase in the performance should be fair for all Release 8,9 and 10 users. This depends on how the operator want to treat the user categories. It also depends on radio resource allocation algorithms that are employed at the eNodeB. Our future works will focus on the optimum carrier allocation using different scheduling algorithms and optimizing the fairness between users supporting different 3GPP Releases simultaneously.

Acknowledgment

This work is supported by Hutchison 3G in the UK.

References

[1] 3GPP, TS 36.201 V8.3.0 ,“Evolved Universal Terrestrial Radio Access (E-UTRA); LTE Physical Layer - General Description,” Rel. 8, Mar. 2009.

[2] 3GPP, TR 36.912 V 10.0.0,“Feasibility study for Further Advancements for EUTRA (LTE-Advanced),” Rel. 10, Mar. 2010.

[3] ITU-R Rec. M.2134, “Requirements Related to Technical Performance for IMT-Advanced Radio Interface(s),” 2008.

[4] 3GPP, TR 36.808 V 1.0.0,“Carrier Aggregation; Base Station (BS) radio transmission and reception ,” Rel. 10, Dec. 2010.

[5] 3GPP,TR 25.825 V1.0.0, “Dual-cell HSDPA operation”, Rel.8, May 2008.

[6] Y. Wang, K. Pedersen, T. andrensen, and P. Mogensen, “Carrier load balancing and packet scheduling for multi-carrier systems,” *IEEE Trans. Wireless Commun.*, vol. 9, no. 5, pp. 17801789, May 2010.

[7] G. Yuan, X. Zhang, W. Wang, and Y. Yang, “Carrier aggregation for LTE-Advanced mobile communication systems,” *IEEE Commun. Magazine*, vol. 48, no. 2, pp. 8893, Feb. 2010.

[8] 3GPP, TR 36.815 V9.1.0, “Further advancements for E-UTRA LTEAdvanced feasibility studies in RAN WG4”, Rel. 10, Jun. 2010.

[9] H. Holma and A. Toskala, *LTE for UMTS OFDM and SC-FDMA based radio acess*, 1st ed. John Wiley and Sons, 2009.

[10] P. B. M. Jeruchim and K. Shanmugan, *Simulation of Communication System Modeling, Methodology, and Techniques*, 2nd ed. Kluwer Acadimic/Plenum, 2000.

[11] P. V. Mieghem, *Performance Analysis of Communications Networks and Systems*, 1st ed. Cambridge University Press, 2006.

[12] S. Plass, X. G. Doukopoulos, and R. Legouable, “Investigations on link-level inter-cell interference in OFDMA systems,” in *Symp. Commun. and Veh. Technology*, pp. 4952, Nov. 2006.

[13] A. Krishnamoorthy, Y. Blankenship, P. Sartori, K. Baum, and B. Classon, “Enhanced link adaptation methods for wireless multi-carrier systems,” *Proc. IEEE VTC2007-Spring*, pp. 19111915, Apr. 2007.

[14] 3GPP, WG1 R1-061506,“System analysis of the impact of CQI reporting period in DL SIMO OFDMA,” V7.1.0, May 2006.

[15] A. Jalali, R. Padovani, and R. Pankaj, “Data throughput of CDMA-HDR a high efficiency-high data rate personal communication wireless system,” in *Proc. IEEE VTC00-Spring*, May 2000.